NAVAL POSTGRADUATE SCHOOL
Monterey, California

THESIS

FINITE ELEMENT ANALYSIS OF THE HIERARCHICAL STRUCTURE OF HUMAN BONE

by

Katherine M. Dolloff

March 2003

Thesis Advisor: Young W. Kwon

Approved for public release; distribution is unlimited.

THIS PAGE INTENTIONALLY LEFT BLANK

REPORT DOCUMENTATION PAGE		*Form Approved OMB No. 0704-0188*

Public reporting burden for this collection of information is estimated to average 1 hour per response, including the time for reviewing instruction, searching existing data sources, gathering and maintaining the data needed, and completing and reviewing the collection of information. Send comments regarding this burden estimate or any other aspect of this collection of information, including suggestions for reducing this burden, to Washington headquarters Services, Directorate for Information Operations and Reports, 1215 Jefferson Davis Highway, Suite 1204, Arlington, VA 22202-4302, and to the Office of Management and Budget, Paperwork Reduction Project (0704-0188) Washington DC 20503.

1. AGENCY USE ONLY *(Leave blank)*	2. REPORT DATE March 2003	3. REPORT TYPE AND DATES COVERED Master's Thesis	
4. TITLE AND SUBTITLE Finite Element Analysis of the Hierarchical Structure of Human Bone		5. FUNDING NUMBERS	
6. AUTHOR (S) Katherine M. Dolloff			
7. PERFORMING ORGANIZATION NAME(S) AND ADDRESS(ES) Naval Postgraduate School Monterey, CA 93943-5000		8. PERFORMING ORGANIZATION REPORT NUMBER	
9. SPONSORING / MONITORING AGENCY NAME(S) AND ADDRESS(ES)		10. SPONSORING/MONITORING AGENCY REPORT NUMBER	
11. SUPPLEMENTARY NOTES The views expressed in this thesis are those of the author and do not reflect the official policy or position of the U.S. Department of Defense or the U.S. Government.			
12a. DISTRIBUTION / AVAILABILITY STATEMENT Approved for public release; distribution is unlimited.		12b. DISTRIBUTION CODE A	

13. ABSTRACT *(maximum 200 words)*

The objective of this study was to develop an analytical model of the basic hierarchical structure of the human bone. The model computed the stiffness of composite collagen fibers comprised of collagen fibrils and hydroxyapatite mineral crystals. Next, the stiffness of the concentric lamella was computed utilizing the stiffness of the collagen fibers and layer information. Finally, the effective stiffness of the bone was estimated. In order to determine the stiffness of the collagen fiber, a three-dimensional finite element model was developed and a simple analytical model was derived. The simple analytical model was validated using the finite element results. The lamination theory of unidirectional fibrous composites was used to calculate the stiffness of the lamella and eventually the bone stiffness. A series of parametric studies were conducted to understand what parameter(s) affected the stiffness of the bone most significantly. This information will be useful when an artificial bone structure is designed.

14. SUBJECT TERMS Finite Element Analysis, Finite Element Model, Human Bone Modeling, Bone Structure, Lamination Theory			15. NUMBER OF PAGES 61
			16. PRICE CODE
17. SECURITY CLASSIFICATION OF REPORT Unclassified	18. SECURITY CLASSIFICATION OF THIS PAGE Unclassified	19. SECURITY CLASSIFICATION OF ABSTRACT Unclassified	20. LIMITATION OF ABSTRACT UL

NSN 7540-01-280-5500

Standard Form 298 (Rev. 2-89)
Prescribed by ANSI Std. 239-18

THIS PAGE INTENTIONALLY LEFT BLANK

FINITE ELEMENT ANLYSIS OF THE HIERACRHICAL STRUCTURE OF HUMAN BONE

Katherine M. Dolloff
Lieutenant, United States Navy
B.S., United States Naval Academy, 1994

Submitted in partial fulfillment of the
requirements for the degree of

MASTER OF SCIENCE IN MECHANICAL ENGINEERING

from the

NAVAL POSTGRADUATE SCHOOL
March 2003

Author: Katherine M. Dolloff

Approved by: Young W. Kwon
               Thesis Advisor

               Young W. Kwon, Chairman
               Department of Mechanical Engineering

THIS PAGE INTENTIONALLY LEFT BLANK

ABSTRACT

The objective of this study was to develop an analytical model of the basic hierarchical structure of the human bone. The model computed the stiffness of composite collagen fibers comprised of collagen fibrils and hydroxyapatite mineral crystals. Next, the stiffness of the concentric lamella was computed utilizing the stiffness of the collagen fibers and layer information. Finally, the effective stiffness of the bone was estimated. In order to determine the stiffness of the collagen fiber, a three-dimensional finite element model was developed and a simple analytical model was derived. The simple analytical model was validated using the finite element results. The lamination theory of unidirectional fibrous composites was used to calculate the stiffness of the lamella and eventually the bone stiffness. A series of parametric studies were conducted to understand what parameter(s) affected the stiffness of the bone most significantly. This information will be useful when an artificial bone structure is designed.

THIS PAGE INTENTIONALLY LEFT BLANK

TABLE OF CONTENTS

LIST OF FIGURES

THIS PAGE INTENTIONALLY LEFT BLANK

ACKNOWLEDGEMENTS

THIS PAGE INTENTIONALLY LEFT BLANK

I.   INTRODUCTION

This thesis research developed both an analytical model and a finite element model of the hierarchical structure of human bone. The analytical model was validated using the results from the finite element model. Before we delve into the aspects of each model, it is important to understand the structure of the human bone. Figure 1 shows molecular to ultra to micro to macro components of the bone, which will be discussed in the subsequent section.
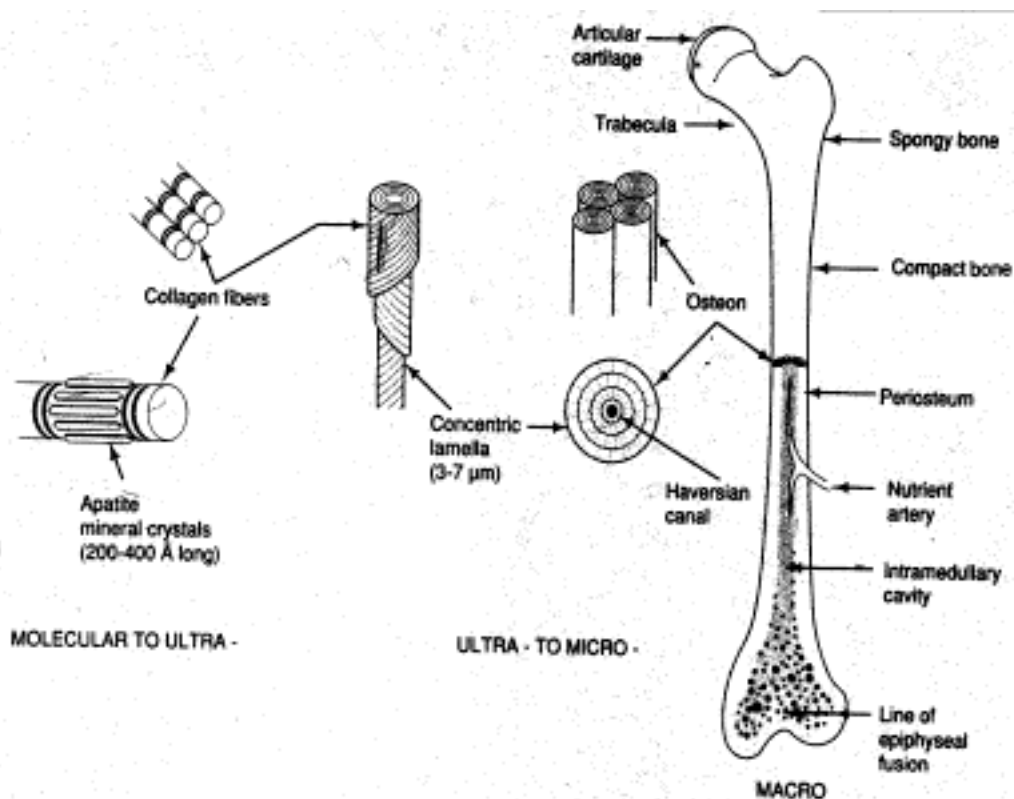
Figure 1.   Hierarchical Structure of Human Bone (From: Rockwood, 2001)

A.   HUMAN BONE STRUCTURE

Starting with the molecular structure of bone we have hydroxyapatite mineral crystals, commonly known as apatite. These mineral crystals provide for the hardness and brittle nature of bone (Apatite, 2001).

The hydroxyapatite lies in sections around a collagen fibril. The collagen has great tensile strength and allows for bone's elastic behavior which complements the properties of the apatite (Collagen, 2001). Together these materials make up the composite fiber and account for the molecular structure of bone.

The ultra component of the bone structure consists of many concentric lamellas. In nature these lamella are oriented 45° from the longitudinal axis. Each layer of the lamellae are at opposing angles and there are 3-20 lamella comprising the lamellae (Caceci, 2001).

The osteon or the Haversion system is the micro component of bone. This is made up of many lamellae encircling an inner region to provide protection. This inner region consists of:

- The Haversion canal which contains one or two small blood vessels and a nerve (Osteon, 2002).

- Lacunae; which are holes for one bone cell (osteocyte) to live (Osteon, 2002).

- Canaliculi which enable osteocytes to communicate with one another (Osteon, 2002).

- Volkman's canal which enables adjacent osteons to communicate with each other (Osteon, 2002).

The macro components of bone make up bone as most of us know it today. As seen in Figure 1, there are many different parts which make up the outer structure of the bone. This research did not account for every one, but instead grouped them together to account for the 30% of bone which was not analyzed with the finite element model or with the analytic predictions. In other words our final values for the properties of bone were based upon the lamella structure and multiplied by 70%.

B.   OBJECTIVES

The objective of this study was to develop an analytical model of the basic hierarchical structure of the human bone, consisting of collagen and hydroxyapatite. The model computed the stiffness of composite collagen fibers comprised of collagen fibrils and hydroxyapatite mineral crystals. Once the model was developed, the stiffness of the concentric lamella was computed utilizing the stiffness of the collagen fibers and layer information. Finally, the effective stiffness of the bone was estimated.

In order to determine the stiffness of the collagen fiber, a three-dimensional finite element model was developed and a simple analytical model was derived. The simple analytical model was validated using the finite element results. The lamination theory of unidirectional fibrous composites was used to calculate the stiffness of the lamella and eventually the bone stiffness. A series of parametric studies were conducted to understand what parameter(s) affected the stiffness of the bone most significantly.

THIS PAGE INTENTIONALLY LEFT BLANK

II. FINITE ELEMENT MODEL

A. MODEL OVERVIEW

A three-dimensional, fixed displacement, finite element model of the most basic human bone structure was developed that is capable of predicting the total stress of the composite fiber and therefore, through analytical calculations, the elastic modulus of the composite fiber. The model is on a nanometer scale and represents one section of the composite fiber, including collagen and hydroxyapatite mineral crystals. The commercial finite element package MSC/PATRAN was used for pre and post processing and MSC/NASTRAN was used for analysis.

B. GEOMETRY

One section of the composite fiber was modeled, as shown in Figure 2. Beginning with a solid cylinder to represent a portion of the collagen fibril, 64 nm in length with a radius of 60 nm, hydroxyapatite mineral crystals, 48 nm in length and 2nm in width, were placed on the outside of the cylinder. These two materials made up the composite collagen fiber. The elastic modulus of each component was varied in order to analyze the individual effect on the elastic modulus of the composite. The stiffness of collagen was adjusted from 10 to 30 GPa at 5 GPa intervals. Separately, the stiffness of hydroxyapatite was adjusted from 700 GPa to 450 GPa at 50 GPa intervals. These values were chosen at random to determine the trend of the composite stiffness as each value was changed.
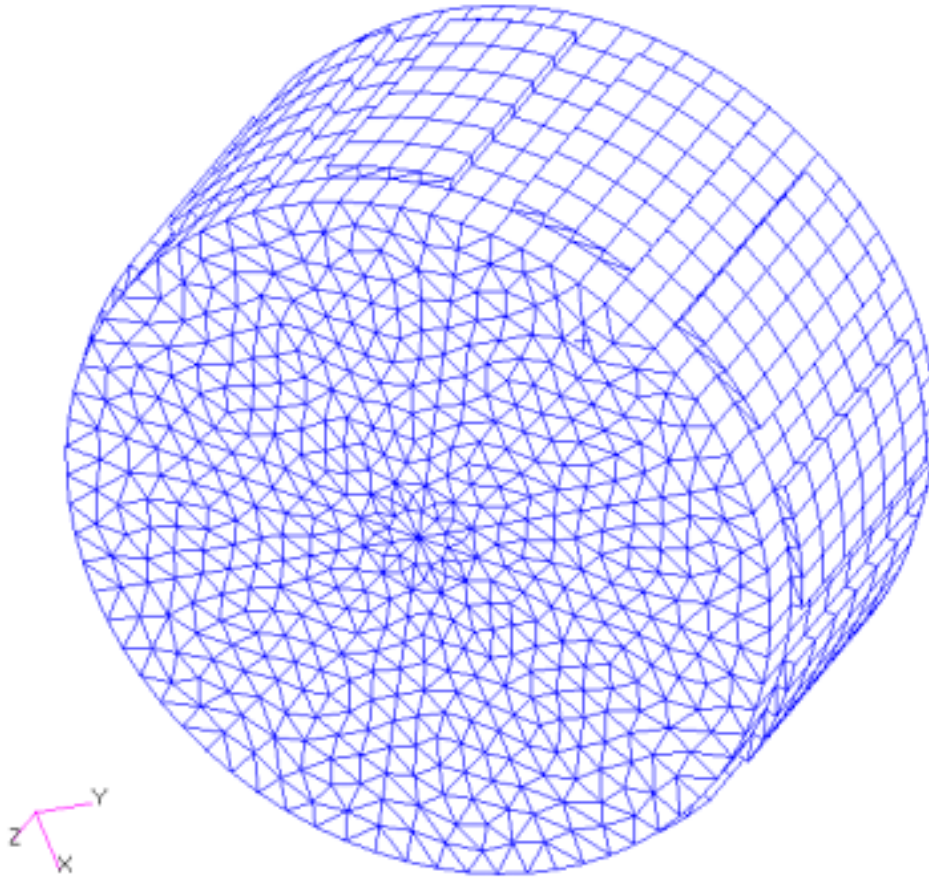
Figure 2.   Finite Element Model of Composite Fiber

C.   STATIC RESPONSE

The finite element model was run multiple times with different values for the elastic modulus of collagen and hydroxyapatite to determine which material affected the elastic modulus of the composite most dramatically. Applying boundary conditions enabled us to fix the translation in the x-direction, fix the translation in the y-direction, and fix rotation in all directions. Applying a fixed displacement to the model in the z-direction, we were able to determine the stress at each point of the composite fiber. Through analytic calculations, we then determined the average stress over the cross sectional

area, to ultimately obtain the elastic modulus of the composite fiber $\left(E = \dfrac{\sigma}{\varepsilon} \right)$, where E = elastic modulus, σ = stress, and ε = strain. Once these results were tabulated we used them to validate our analytic model.

Figure 3 is an example of the output of the model when $E_{apatite}$ = 450 GPa and $E_{collagen}$ = 20 GPa. The various colors represent the stresses on the given portion of the composite material. The analytic calculations to determine the average stress were accomplished on the cross sectional area (face of the fiber). The model is on a nanometer scale, so to obtain a meaningful value, we need to divide each stress value by the average stress over the cross sectional area to obtain the stress concentration. For example, the white value for stress is 2.79e-11 N/nm^2 which when converted to common dimensions, becomes 2.79e7 N/m^2 or 27.9 MPa. We divide this value of stress by the average stress obtained through earlier calculations and obtain, 6.50 stress per unit stress, the stress concentration. This value is explained to give the reader a general idea of what they are seeing in Figure 3, and will make more sense when we discuss our results.
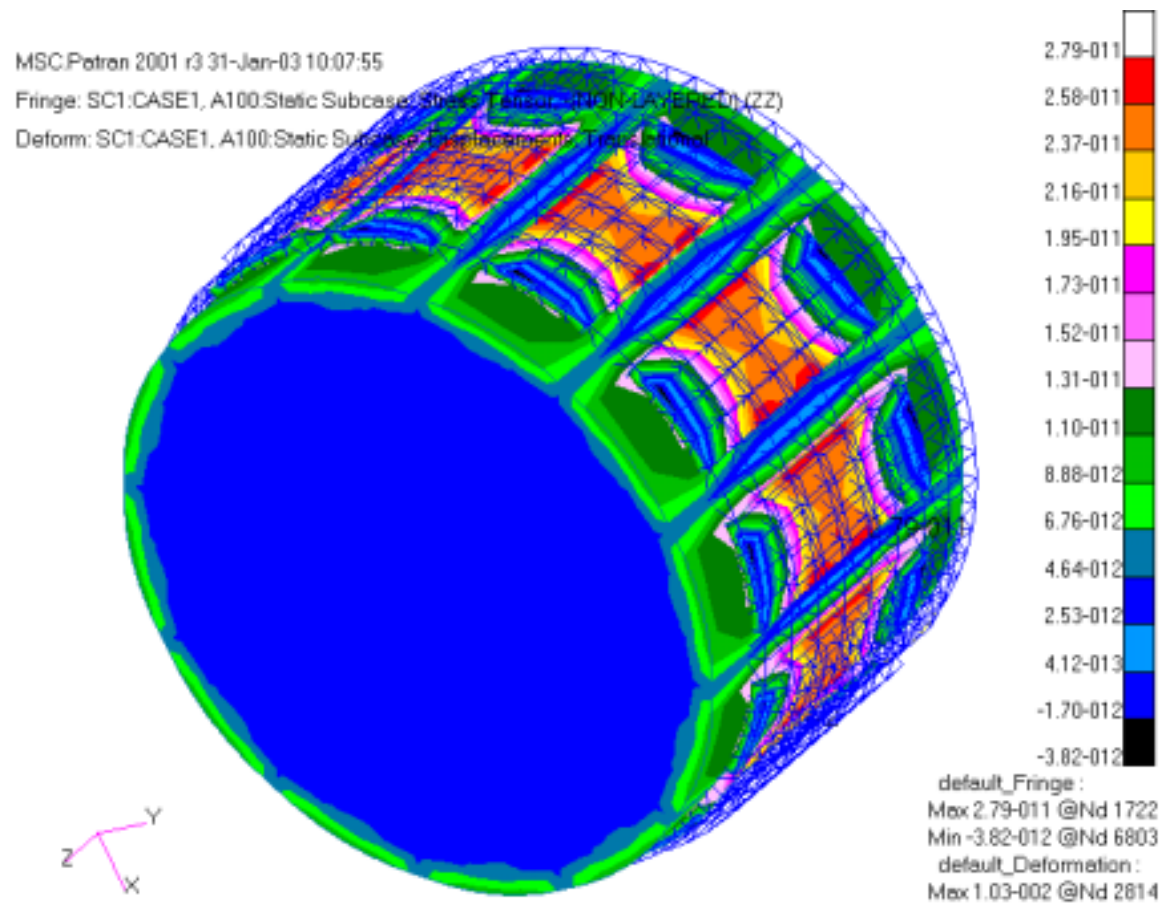
Figure 3.   Stress over Composite

        From the finite element model, we gained insight into
the composite fiber properties and used the results to
validate a simple analytic model.

III. ANALYTIC SOLUTION

An analytic model was derived in a sequence of three separate computer programs. The first computed the stiffness of composite collagen fibers comprised of collagen fibrils and hydroxyapatite mineral crystals. Once this analytic model was validated against the results of the finite element model, the stiffness of the concentric lamella was computed utilizing the stiffness of the collagen fibers and layer information. Finally, the effective stiffness of the bone was estimated.

A. FORCE-DEFORMATION BEHAVIOR OF A TYPICAL UNIFORM AXIAL-DEFORMATION ELEMENT

An analytic model was derived and the results from the finite element model were used as validation for this model. As a starting point, a MATLAB computer program using uniform axial deformation (spring constant) theory was developed. It enabled the user to change the values for the elastic modulus of hydroxyapatite and collagen to determine the longitudinal stiffness of the composite fiber. Figure 4 shows a schematic of the composite fiber.
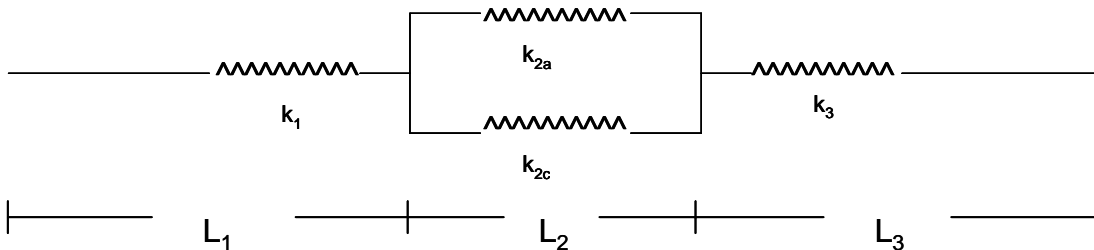
Figure 4.   Spring Constant Schematic of Composite Fiber

We can compare Figure 4 to Figure 5 to see how the spring model correlates to the composite model.
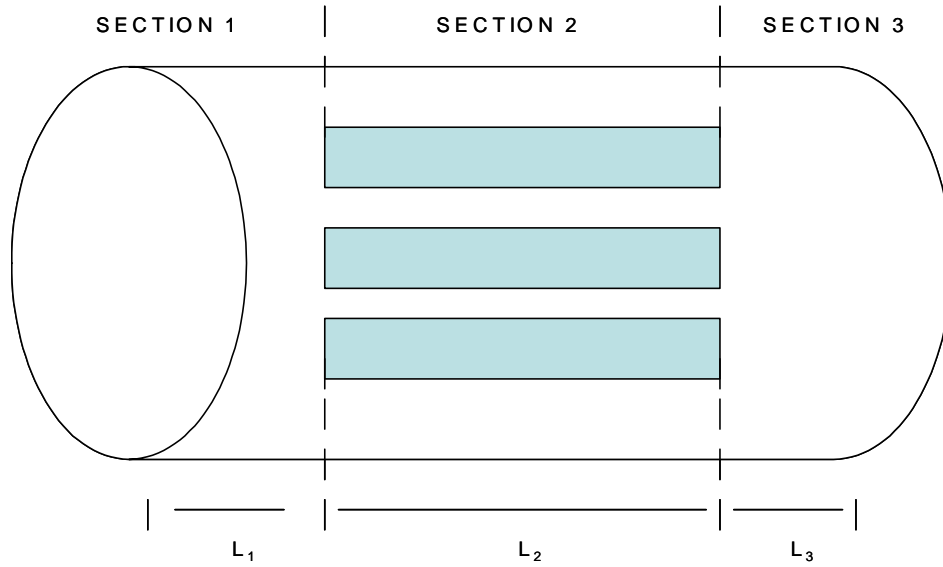
Figure 5.   2-D Finite Element Model Schematic Showing Sections

The basic theory behind this solution is

$$\frac{1}{k} = \frac{1}{k_1} + \frac{1}{k_2} + \frac{1}{k_3}$$

termed the force-deformation behavior of a typical uniform axial-deformation element (Craig, 2000); where k = the total stiffness coefficient (force required to produce a unit elongation of the member), k_1 = the stiffness coefficient for the first section of composite, k_2 = the stiffness coefficient for the second section of the composite, and k_3 = the stiffness coefficient for the third section of the composite. Note that $k_2 = k_{2a} + k_{2c}$ and that k_{2a} = hydroxyapatite stiffness coefficient for the second section and k_{2c} = the collagen stiffness coefficient for the second section.   Solving this equation for k we find

10

$$k = \frac{k_1 k_2 k_3}{k_1 k_2 + k_2 k_3 + k_1 k_3}$$

and from theory we know that $k = \dfrac{AE}{L}$, where A = Area. We substitute this definition for k, into the composite formula and find

$$k_1 = \left(\frac{A_1 E_c}{L_1} \right) = \frac{\pi r^2 E_c}{L_1}$$

$$k_3 = \left(\frac{A_3 E_c}{L_3} \right) = \frac{\pi r^2 E_c}{L_3}$$

but the solution for k_2 is somewhat more involved as it has to be treated as a composite material. In determining k_2 we analyze a cross section of the mineral crystal represented in figure 6, where σ=normal stress, τ=shearing stress, $d\sigma$=change in normal stress, dz=length of the cross section, and s=width and height of cross section.
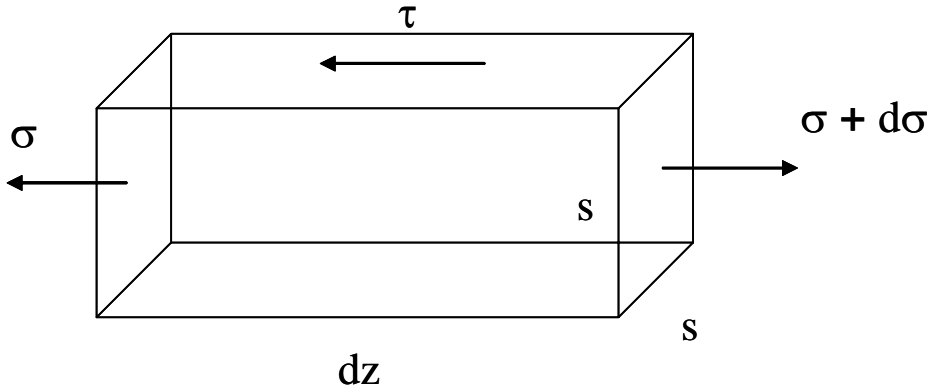
Figure 6.   Cross section of Hydroxyapatite

The first step is to sum the forces over the cross section, and from statics we know that $\sum F = 0$ and $\sigma = \dfrac{F}{A}$. Utilizing

11

this, we find that $\sum F = (\sigma + d\sigma)s^2 - \sigma s^2 - \tau sdz = 0$. Simplifying

this equation and integrating we find that $\sigma(z) = \sigma_o + \dfrac{\tau z}{s}$ where

$\sigma_o = 0$ as there is no stress at the end of the cross section.

Assuming that τ is constant, $\sigma = \dfrac{\tau z}{s}$ and the maximum stress

occurs at the center of the section, as seen in figure 7,
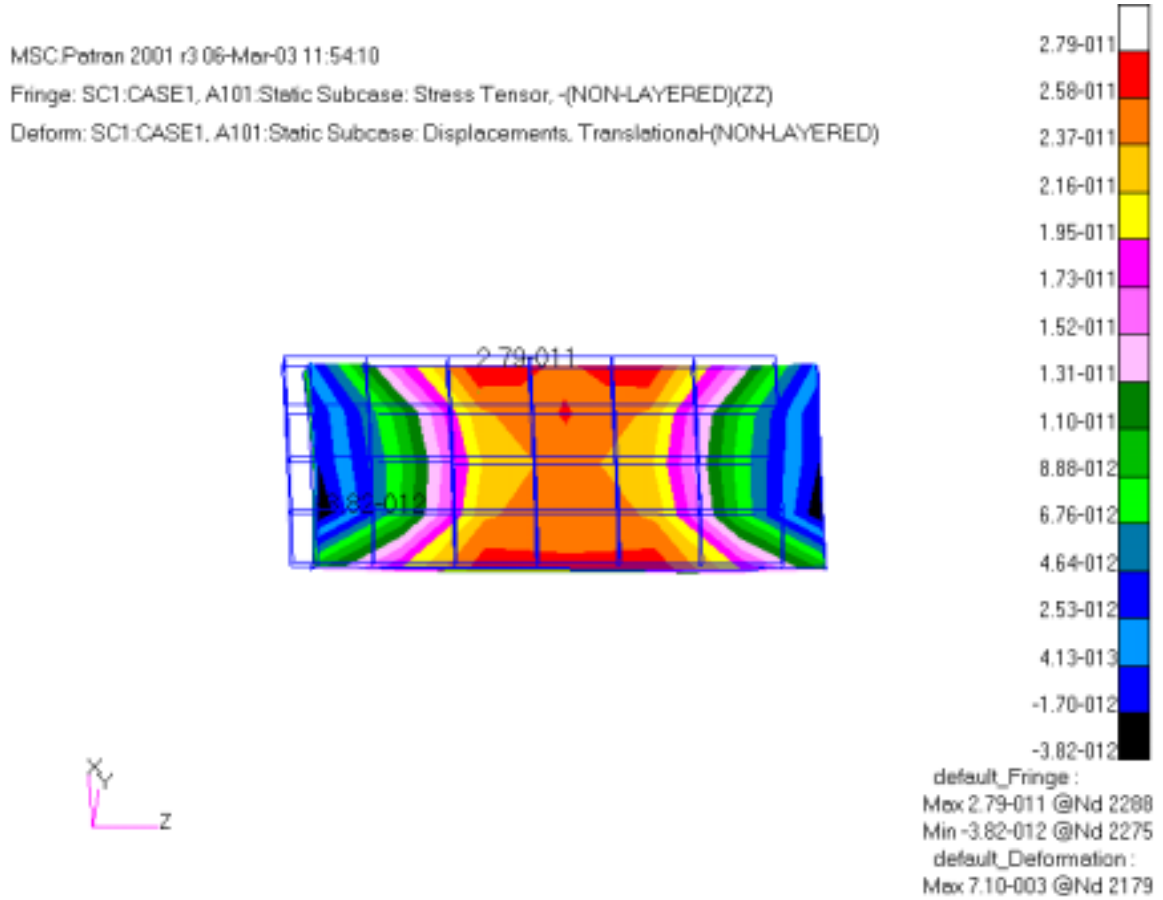
Figure 7.   Stress Over One Section of Hydroxyapatite

therefore, $\sigma_{max} = \dfrac{\tau l}{2s}$ and $\sigma_{avg} = \dfrac{1}{2}\sigma_{max} = \dfrac{1}{2}\dfrac{\tau l}{2s} = \dfrac{\tau l}{4s}$.   Figure 8

represents the shear stress over one section.
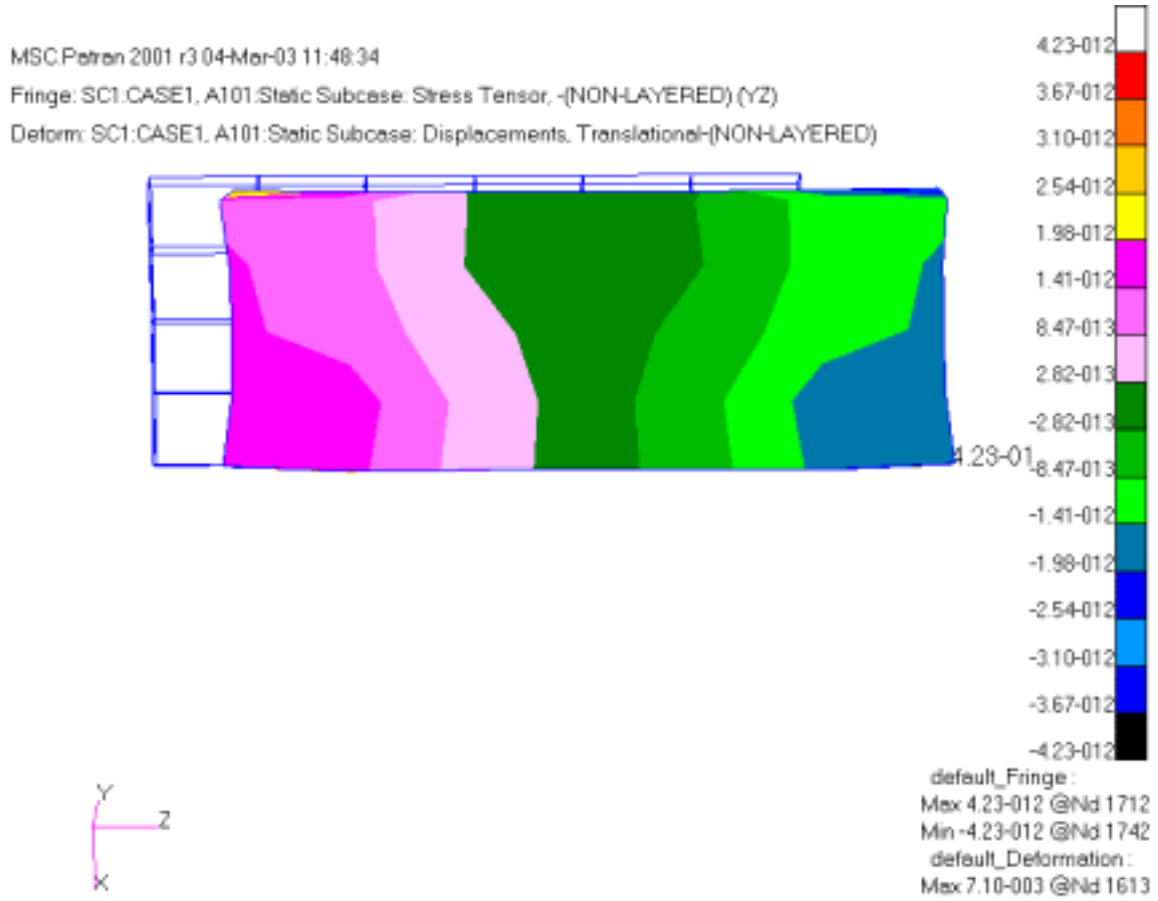
Figure 8.   Shear Stress Over One Section of
Hydroxyapatite

From figures 7 and 8 we find that $F_{avg} = \sigma_{avg} A = \dfrac{\tau ls}{4} = \dfrac{F_{shear}}{4}$.   From
this equation we determine that our value for k_{2a} must have
a factor of 0.25 in the equation, therefore,

$$k_2 = \left(\frac{A_a E_a}{L_2}\right) + \left(\frac{A_c E_c}{L_2}\right) = \left(\frac{nA_a E_a}{4L_2}\right) + \left(\frac{\pi r^2 E_c}{L_2}\right)$$

where r = radius, the c subscript represents collagen, the
a subscript represents apatite, and n = the number of
sections of apatite around the fibril.   We can now

13

determine k, which in turn enables us to determine the elastic modulus of the composite fiber, using

$$E_{composite} = \frac{kL}{\pi r^2}$$

The value obtained here for E$_{composite}$, is the longitudinal elastic modulus of the composite fiber. The results from this analytic process were used to validate our model and as a basis to move on to the next step which was to find the elastic modulus of the composite fiber when oriented at various angles.

B.   LAMINATION THEORY OF UNIDIRECTIONAL FIBROUS COMPOSITES

The lamination theory of unidirectional fibrous composites was utilized to derive the next portion of the analytic model. The value for the longitudinal elastic modulus of the composite fiber was the starting point. This value was used in the transformed stiffness matrix to produce the elastic modulus of a single fiber oriented at various angles. The angles of orientation included 15°, 30°, 45°, 60°, -15°, -30°, -45°, and -60°.

The following stress-strain relations for isotropic materials were used (Jones, 1975):

$$\begin{Bmatrix} \sigma_1 \\ \sigma_2 \\ \tau_{12} \end{Bmatrix} = \begin{bmatrix} Q_{11} & Q_{12} & 0 \\ Q_{12} & Q_{22} & 0 \\ 0 & 0 & Q_{66} \end{bmatrix} \begin{Bmatrix} \varepsilon_1 \\ \varepsilon_2 \\ \gamma_{12} \end{Bmatrix}$$

in which Q_{ij} are the reduced stiffnesses; specifically, $Q_{11} = \frac{E}{1-\upsilon^2}$ where υ is Poisson's ratio and assumed to be 0.3, and Q_{12}, Q_{22}, and Q_{66} are all zero. Using these results, we

14

then calculated the transformed reduced stiffnesses using the following stress-strain relations in the xy coordinate directions (Jones, 1975):

$$\left\{\begin{array}{c} \sigma_x \\ \sigma_y \\ \tau_{xy} \end{array}\right\} = \left[\begin{array}{ccc} \overline{Q}_{11} & \overline{Q}_{12} & \overline{Q}_{16} \\ \overline{Q}_{12} & \overline{Q}_{22} & \overline{Q}_{26} \\ \overline{Q}_{16} & \overline{Q}_{26} & \overline{Q}_{66} \end{array}\right] \left\{\begin{array}{c} \varepsilon_x \\ \varepsilon_y \\ \gamma_{xy} \end{array}\right\}$$

in which $\overline{Q}_{ij}$ are the transformed reduced stiffnesses; specifically (Jones, 1975),

$$\overline{Q}_{11} = Q_{11} \cos^4\theta + 2\left(Q_{12} + 2Q_{66}\right)\sin^2\theta\cos^2\theta + Q_{22}\sin^4\theta$$

$$\overline{Q}_{12} = \left(Q_{11} + Q_{22} - 4Q_{66}\right)\sin^2\theta\cos^2\theta + Q_{12}\left(\sin^4\theta + \cos^4\theta\right)$$

$$\overline{Q}_{22} = Q_{11}\sin^4\theta + 2\left(Q_{12} + 2Q_{66}\right)\sin^2\theta\cos^2\theta + Q_{22}\cos^4\theta$$

$$\overline{Q}_{16} = \left(Q_{11} - Q_{12} - 2Q_{66}\right)\sin\theta\cos^3\theta + \left(Q_{12} - Q_{22} + 2Q_{66}\right)\sin^3\theta\cos\theta$$

$$\overline{Q}_{26} = \left(Q_{11} - Q_{12} - 2Q_{66}\right)\sin^3\theta\cos\theta + \left(Q_{12} - Q_{22} + 2Q_{66}\right)\sin\theta\cos^3\theta$$

$$\overline{Q}_{66} = \left(Q_{11} + Q_{22} - 2Q_{12} - 2Q_{66}\right)\sin^2\theta\cos^2\theta + Q_{66}\left(\sin^4\theta + \cos^4\theta\right)$$

The transformed elastic modulus of the composite fiber was equivalent to $\overline{Q}_{11}$. This value was then used as a starting point in the last step of the analytic model derivation to determine the actual elastic modulus of human bone.

C.   LAMELLAE AND BONE ELASTIC MODULUS

Considering actual human bone structure, the composite fibers were wrapped in a concentric lamella, each oriented at opposing angles. From the previous section, we determined the elastic modulus of a given composite fiber oriented at a given angle. The last step in the sequence

to derive the analytic model started with these results and determined first, the elastic modulus of the lamellae structure, and second, the elastic modulus of bone.

The lamellae was assumed to have 12 layers, as an average between the 3-20 lamella stated in the references (Caceci, 2001). The transformed elastic modulus for each angle (15°, 30°, 45°, 60°, -15°, -30°, -45°, and -60°), from the previous derivation using the transformed matrix, was the starting point. Radius and area $\left(A = \pi r^2\right)$ calculations were made for each layer of the concentric lamella as well as for the total area of the lamellae. To calculate the elastic modulus of the entire lamellae, the following formula was used:

$$\frac{\sum_{i=1}^{12} A_i E_{angle}}{TotalArea}$$

Once the stiffness of the lamellae was obtained, the only thing which remained was to make an estimate to determine the actual stiffness of the entire bone. To do this, we assumed that the lamellae represented 70% of the human bone structure. We multiplied the lamellae stiffness by 0.7 to account for this 70% and obtained the elastic modulus of human bone.

IV. RESULTS AND DISCUSSION

A. EFFECT OF ELASTIC MODULUS OF COLLAGEN AND HYDROXYAPATITE ON STRESS CONCENTRATION OF COMPOSITE FIBER

From the figures below we determine that the elastic modulus of collagen has a similar impact on the stress concentration of the composite fiber as the elastic modulus of hydroxyapatite, although collagen may be somewhat more influential. The stress results of the finite element model enabled us to determine the stress concentration over the composite fiber utilizing the following formula:

$$StressConcentration = \frac{LocalizedHighStress}{UniformStressoverRemainder} = \frac{\sigma_{max}}{\sigma_{avg}}$$

1. Effect of Elastic Modulus of Collagen on Stress Concentration of Composite Fiber

Figure 9 shows how the stress concentration over the composite fiber decreases as the stiffness of collagen increases. This decrease is as expected because as the stiffness of collagen increases its value gets closer to the stiffness of apatite. From theory, the closer the stiffness of the two materials, the lower the stress concentration should be (Ugural, 1995). The results shown in Figure 9 agree with theory.

17

Stress Concentration vs E collagen
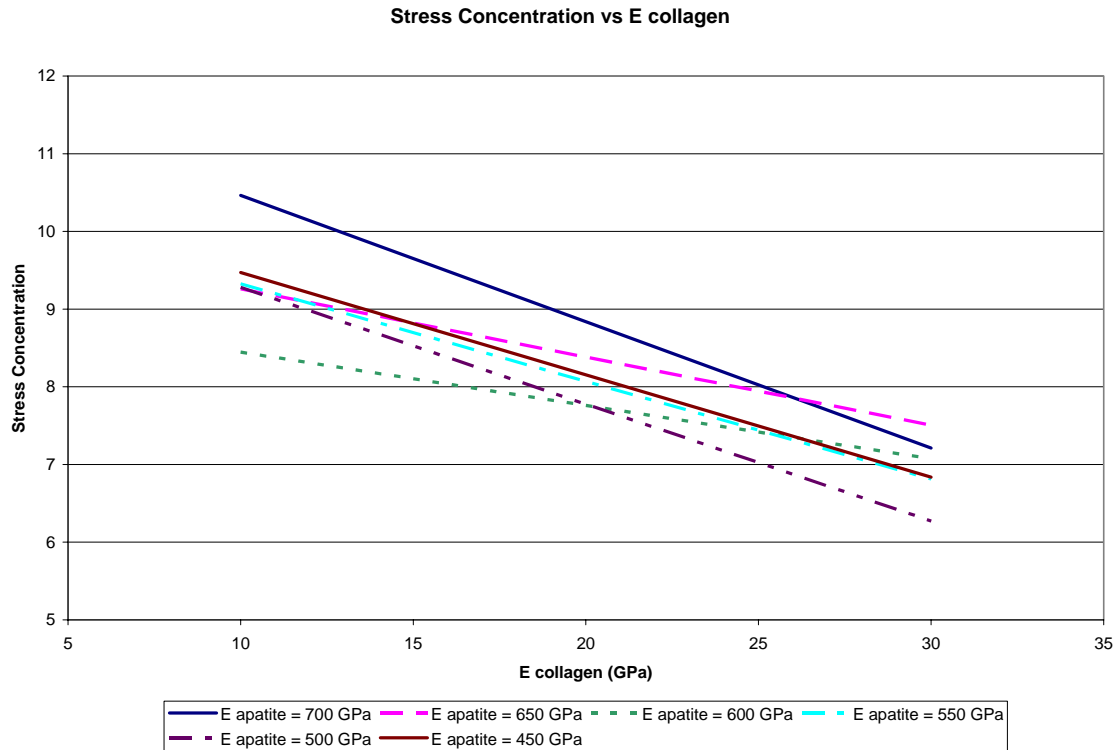
Figure 9.   Effect of Varying Elastic Modulus of Collagen
                   on Stress Concentration

2.   Effect of Elastic Modulus of Hydroxyapatite on Stress Concentration of Composite Fiber

Figure 10 shows that as the stiffness of apatite increases, the stress concentration increases or maintains its approximate value. As with Figure 9, these results agree with theory because as you increase the stiffness of apatite you are moving farther away from the stiffness of collagen, thereby increasing the stress concentration.
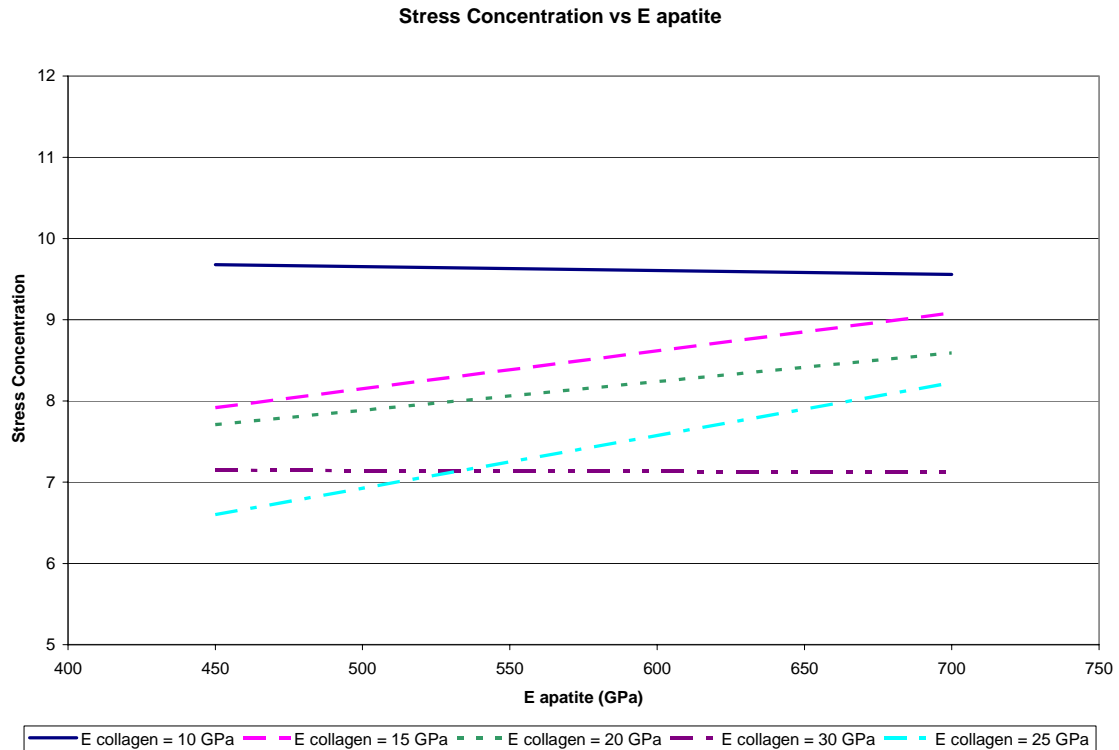
18

Stress Concentration vs E apatite

Figure 10.   Effect of varying Elastic Modulus of
Hydroxyapatite on Stress Concentration

When analyzing Figure 9 and 10 together, we can look
at the ratio of change of the stress concentration.   For
example, beginning with Figure 9 and a collagen stiffness
of 10 GPa (with $E_{apatite}$ = 700 GPa) the stress concentration
is 10.5, a 50% change in collagen stiffness would give us
15 GPa and a stress concentration of 9.5.   So there is one
unit of change in stress concentration with a 50% change in
collagen stiffness.   Now, looking at Figure 10, and an
apatite stiffness of 450 (Ecollagen = 15 GPa) the stress
concentration is 8, a 50% change in apatite stiffness would
give us 675 GPa and a stress concentration of 9.   Here
there is also one unit of change in stress concentration
with a 50% change in apatite stiffness.

19

B. EFFECT OF ELASTIC MODULUS OF COLLAGEN AND HYDROXYAPATITE ON COMPOSITE ELASTIC MODULUS

Figures 11 and 12 show the effect of varying the elastic modulus of hydroxyapatite and collagen on the resulting elastic modulus of the composite. As discussed below, the changes in collagen have a much greater impact on the composite than do the changes in hydroxyapatite.

1. Effect of Elastic Modulus of Collagen on Elastic Modulus of Composite

Figure 11 shows as the elastic modulus of hydroxyapatite is kept constant, the elastic modulus of the composite increases linearly as the elastic modulus of collagen increases.
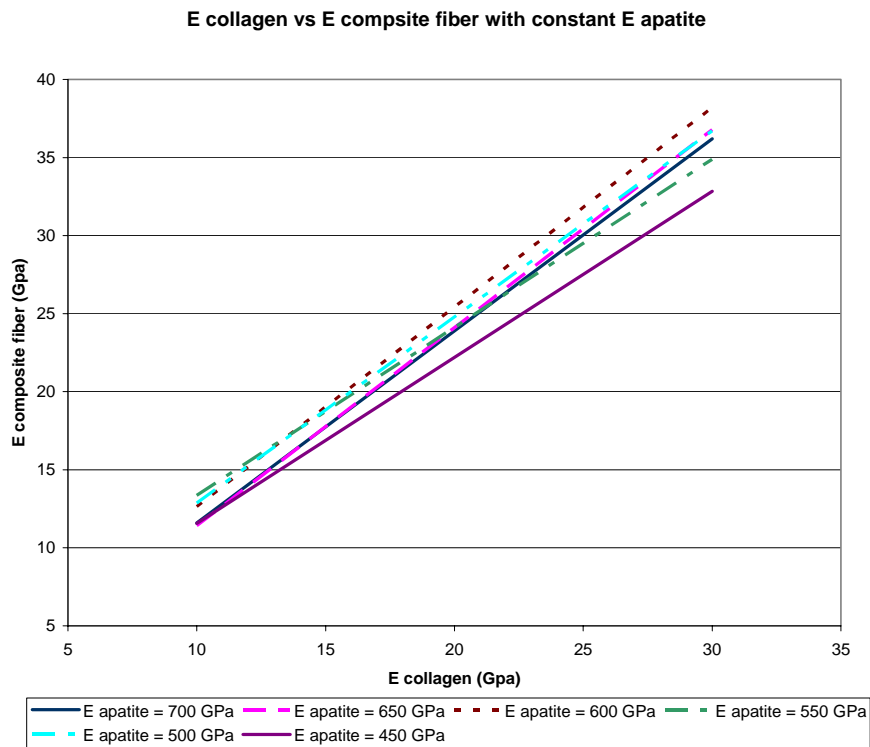

Figure 11.   Effect of Collagen Elastic Modulus on Composite Elastic Modulus

Six different values for the hydroxyapatite elastic modulus
are shown with each line on the graph.

**2.   Effect of Elastic Modulus of Hydroyapatite on
        Elastic Modulus of Composite**

Figure 12 shows the slight increase of the elastic
modulus of the composite as the elastic modulus of
hydroxyapatite is increased.

E apatite vs E composite fiber with constant E collagen
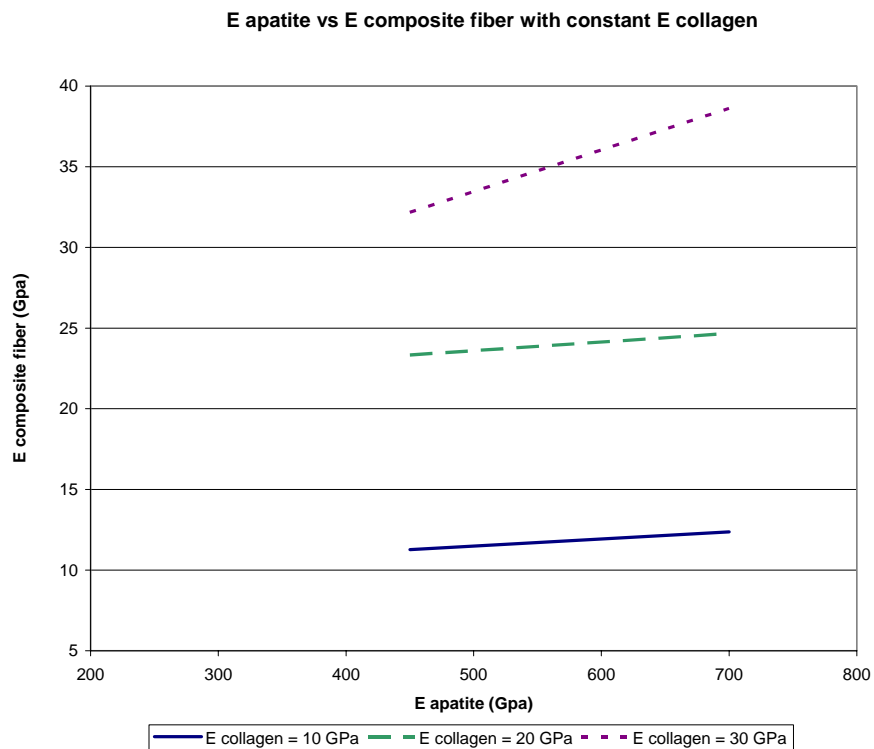

Figure 12.   Effect of Hydroxyapatite Elastic Modulus on
              the Composite Elastic Modulus

The plot shows three different values for the elastic
modulus of collagen with each different line. We see that
varying the elastic modulus of hydroxyapatite does not have
a dramatic effect on the resulting properties of the
composite material.

21

C. FINITE ELEMENT MODEL COMPARED TO AXIAL DEFORMATION CALCULATIONS

After utilizing the finite element model to obtain values for the elastic modulus of the composite, we wanted to validate our simple analytic model using this data. Figures 13-18 plot the FEM data with our analytic data from axial deformation calculations. Both results compare very well.

1. Constant Collagen Elastic Modulus

Figures 13-15 show the proximity of our finite element model calculations to the analytic data obtained from axial deformation calculations when varying the elastic modulus of hydroxyapatite. Errors are likely due to approximations and hand calculations used to obtain average stress results from the finite element model.

Figure 13, specifically shows the difference between the FEM and analytic data for $E_{collagen}$ = 10 GPa. Note that the lines have the same slope and are within reasonable tolerances of each other.

Figure 13.   FEM vs Analytic Data for $E_{collagen}$ = 10 GPa

Figure 14, specifically shows the difference between the FEM and analytic data for $E_{collagen}$ = 20 GPa. The lines are almost right on top of each other, showing excellent correlation between the FEM data and the analytic calculations.

FEM vs Analytic (E collagen = 20 GPa)
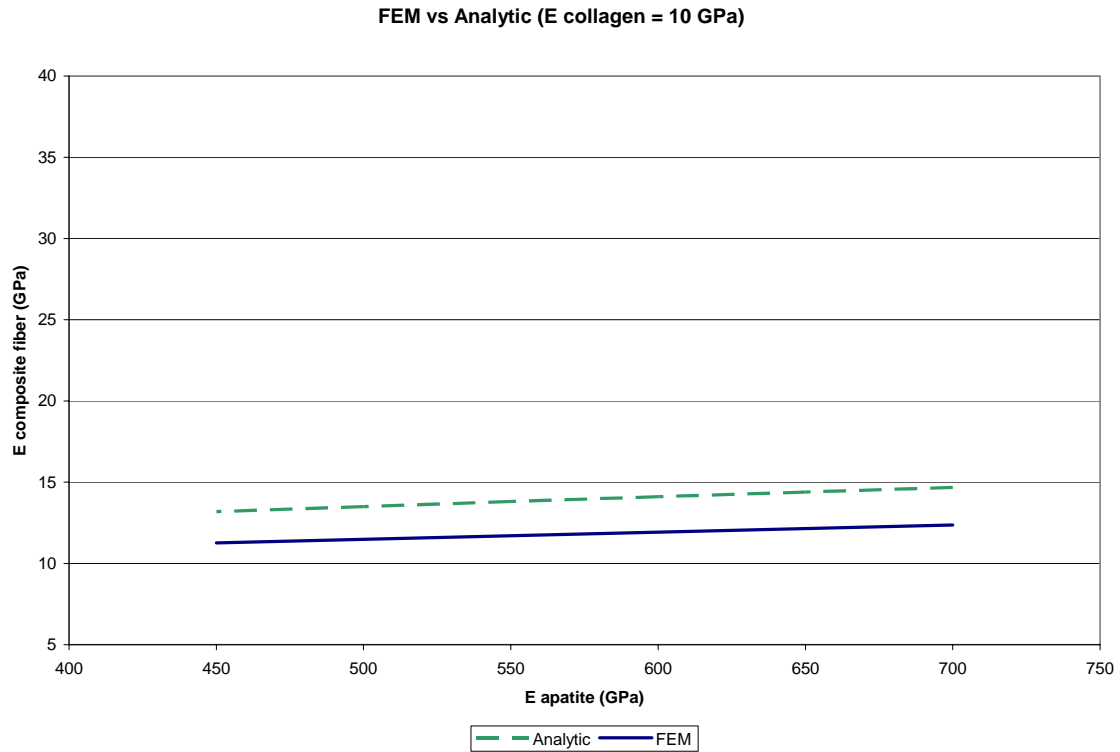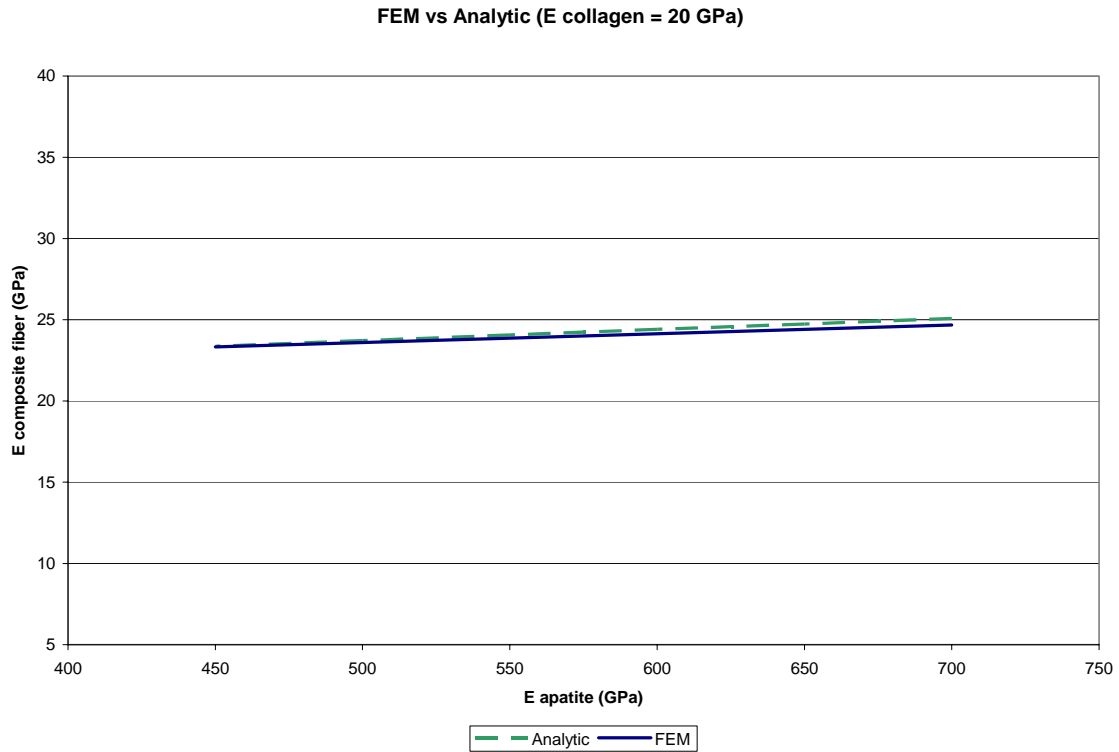

Figure 14.   FEM vs Analytic Data for $E_{collagen}$ = 20 GPa

Figure 15, specifically shows the difference between the FEM and analytic data for $E_{collagen}$ = 30 GPa. This graph shows a bit more deviance from the FEM data to the analytic data, most likely due to the error in approximating the average stress used to find the composite elastic modulus, and due to round off error.

FEM vs Analytic (E collagen = 30 GPa)

Figure 15.   FEM vs Analytic Data for $E_{collagen}$ = 30 GPa

Overall, we determined from Figures 13–15, that when the elastic modulus of collagen is held constant, the FEM and analytic data correlate relatively well.

2.   Constant Hydroxyapatite Elastic Modulus

Figures 16–18 show the proximity of our finite element model calculations to the analytic data obtained from axial deformation calculations when varying the elastic modulus of collagen. Errors are likely due to approximations and hand calculations used to obtain average stress results from the finite element model.

Figure 16, specifically shows the difference between the FEM and analytic data for $E_{apatite}$ = 450 GPa. Again, we see that the values are relatively close.

25

FEM vs Analytic (E apatite = 450 GPa)

Figure 16.   FEM vs Analytic Data for $E_{apatite}$ = 450 GPa

    Figure 17, specifically shows the difference between the FEM and analytic data for $E_{apatite}$ = 550 GPa. As with Figure 14, the lines are almost right on top of each other, showing excellent correlation between the FEM data and the analytic calculations.

FEM vs Analytic (E apatite = 550 GPa)
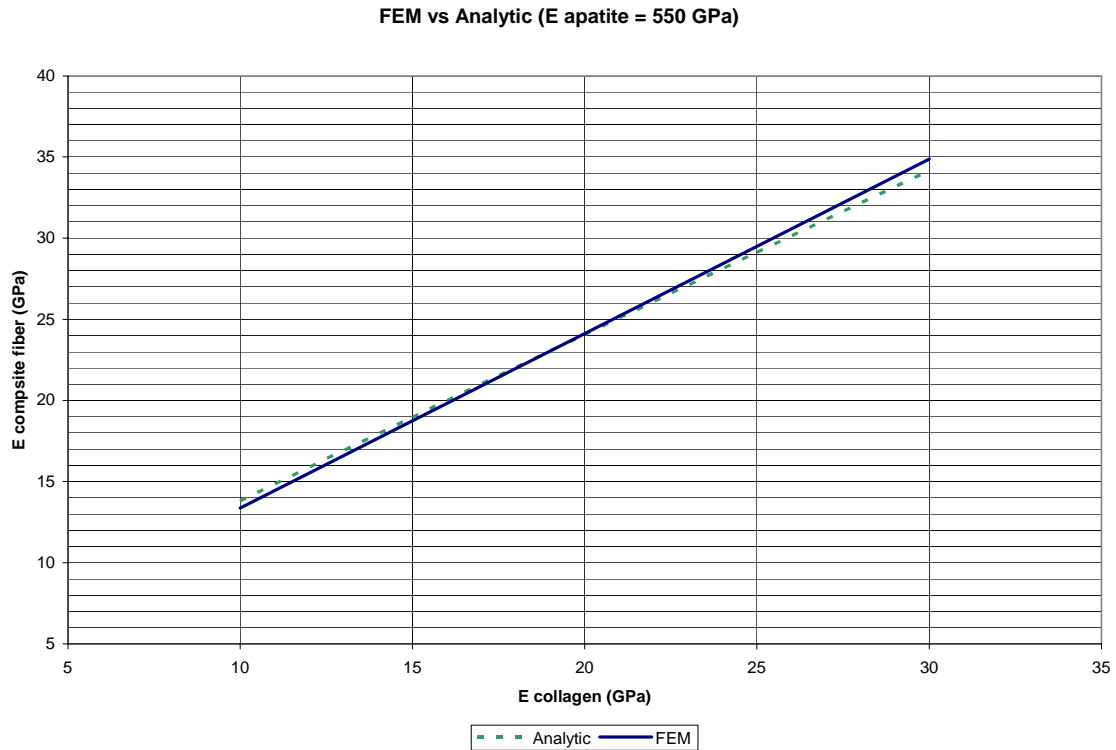
Figure 17.   FEM vs Analytic Data for $E_{apatite}$ = 550 GPa

Figure 18, specifically shows the difference between the FEM and analytic data for $E_{apatite}$ = 650 GPa. As with Figure 15, this graph shows a bit more deviance from the FEM data to the analytic data, most likely due to the error in approximating the average stress used to find the composite elastic modulus, and due to round off error. The values are still relatively close.
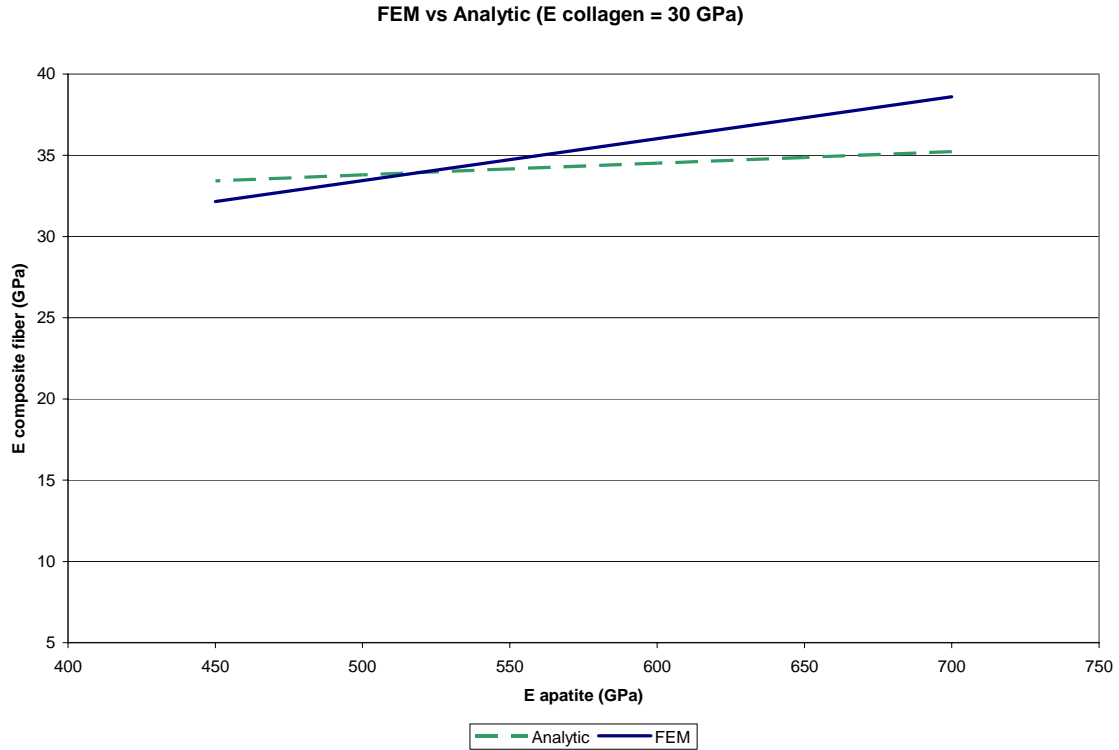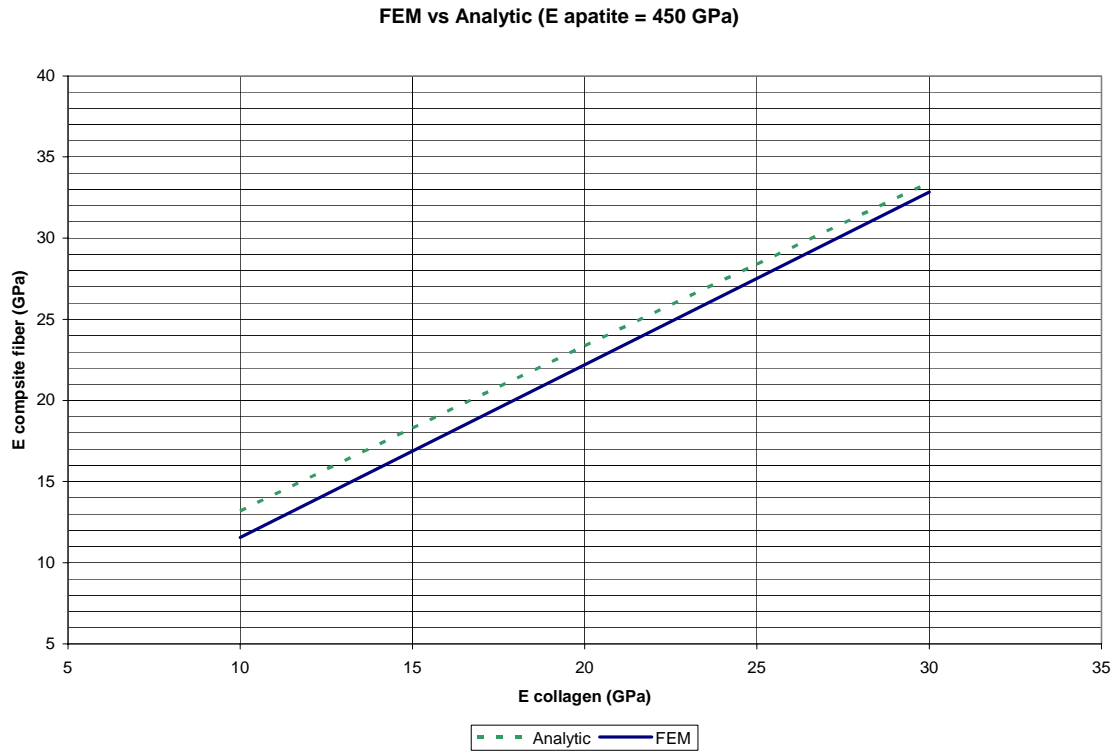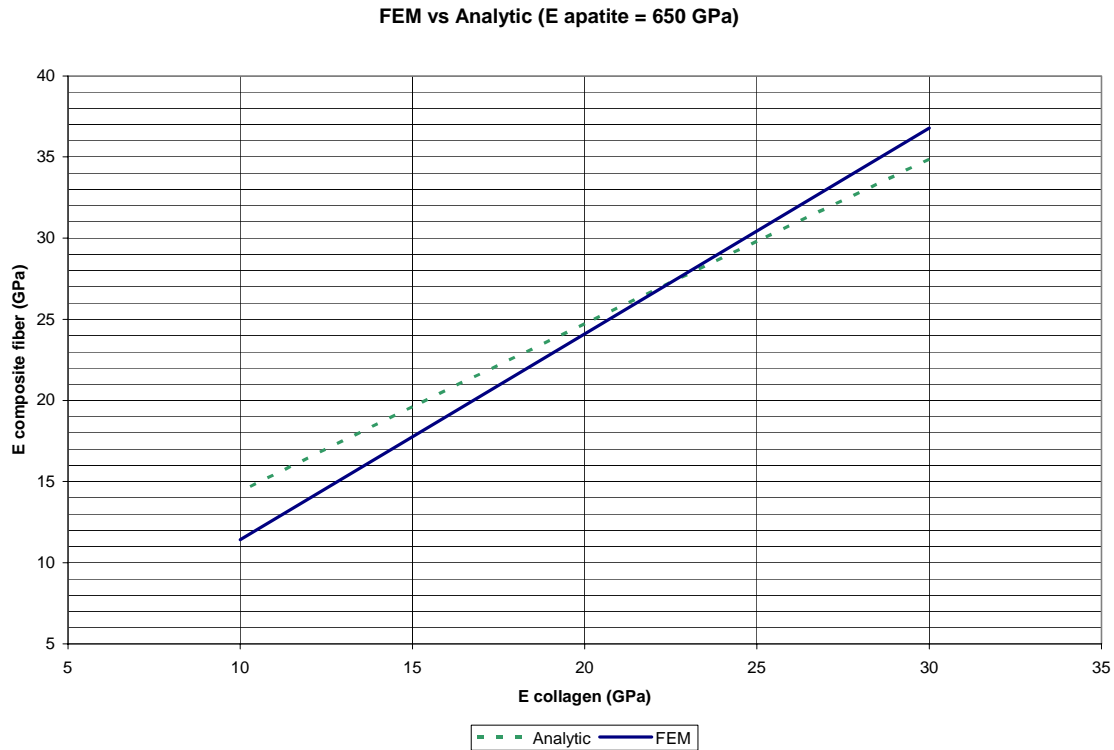
Figure 18.   FEM vs Analytic Data for $E_{apatite}$ = 650 GPa

Overall, we determined from Figures 16-18, that when the elastic modulus of hydroxyapatite is held constant, the FEM and analytic data correlate relatively well.

D.   EFFECT OF VARIOUS LAMELLA ANGLES ON ELASTIC MODULUS OF BONE

Figures 19-24 show the elastic modulus of bone when each layer of the lamellae is oriented at various angles. For example, there are 12 concentric lamella, and the first lamella is oriented at 15°, the second at -15°, the third at 15°, the fourth at -15°, and so on, until you reach the twelfth lamella. Four possible orientations are shown in the graphs in this section.

1.   Constant Collagen Elastic Modulus

Figures 19-21 show the elastic modulus of bone when the lamellae are oriented at various angles and the elastic modulus of collagen is kept constant.   With all three figures it is obvious that the overwhelming contributor to the elastic modulus of bone, is the elastic modulus of collagen.

E bone effected by lamella angles (E collagen = 10 GPa)

Figure 19.   Bone Elastic Modulus with $E_{collagen}$ = 10 GPa

Figure 19, specifically addresses the case when $E_{collagen}$ = 10 GPa.   We see that the various values for the elastic modulus of bone are similar for each value of hydroxyapatite, but as the degree of orientation is increased, the bone elastic modulus decreases, as expected.

The increasing angle of orientation moves each lamella further away from its strictly longitudinal configuration, and therefore causes the bone elastic modulus to continue to decrease. With collagen being so soft, the stiffness of bone remains relatively low for each value of $E_{apatite}$.

E bone effected by lamella angles (E collagen = 20 GPa)
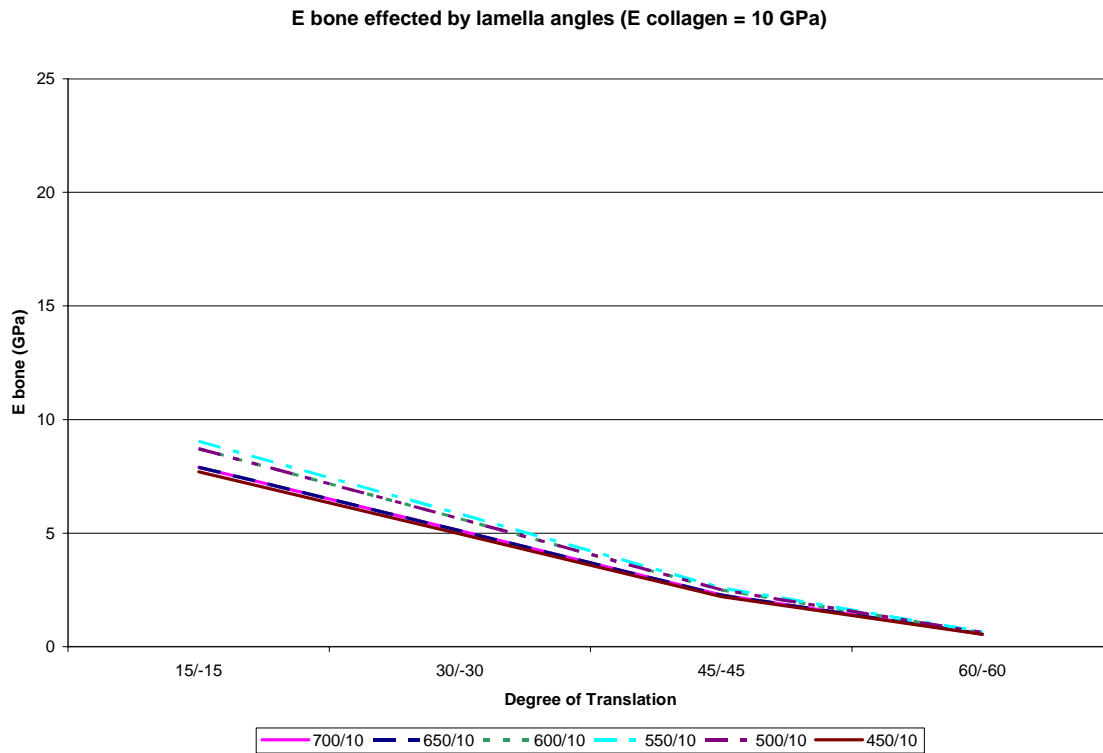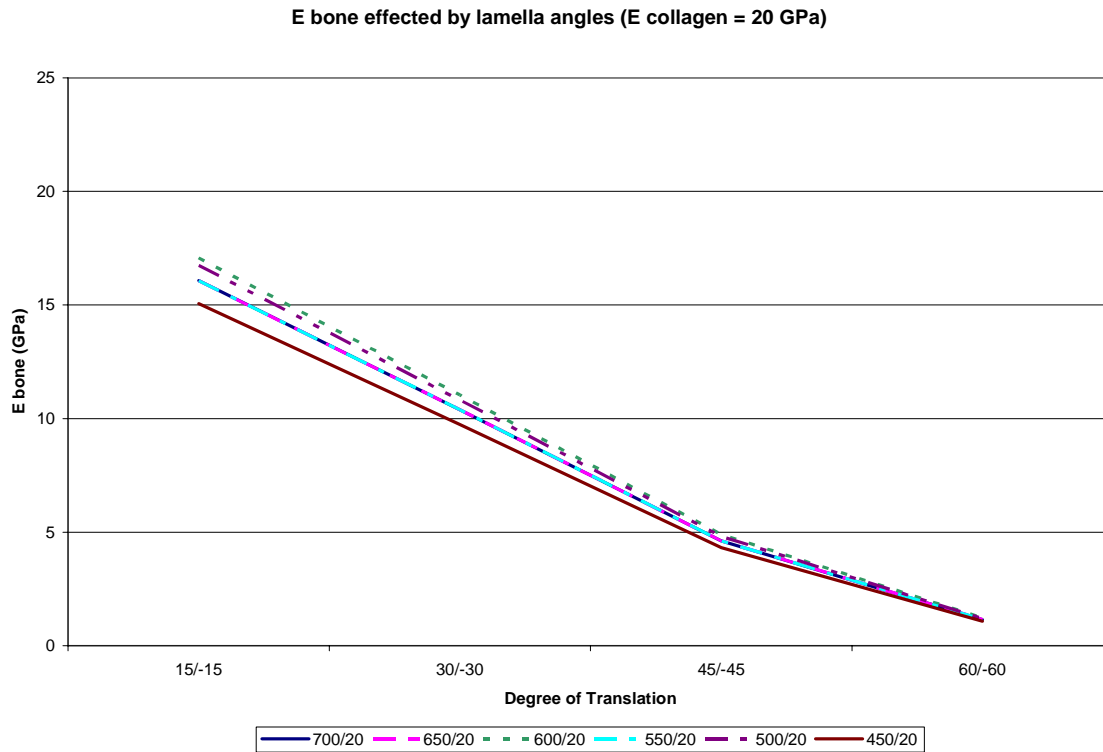

Figure 20.   Bone Elastic Modulus with $E_{collagen}$ = 20 GPa

Figure 20, specifically addresses the case when $E_{collagen}$ = 20 GPa. The same trend in E_{bone} is recognized. The further away from zero degrees the lamella orientation gets, the lower the value for bone elastic modulus. We can see what a difference the harder collagen (E = 20 GPa vice E = 10 GPa) makes on the bone elastic modulus when comparing Figure 20 to Figure 19.

E bone effected by lamella angles (E collagen = 30 GPa)
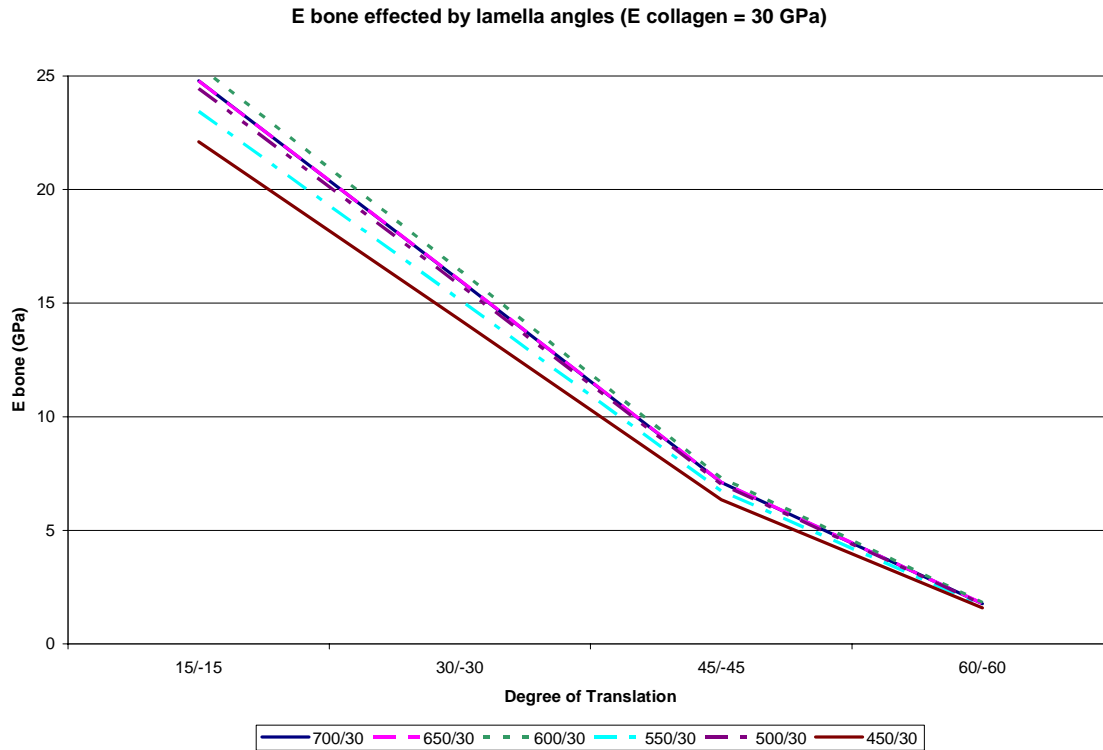
Figure 21.   Bone Elastic Modulus with $E_{collagen}$ = 30 GPa

Figure 21, shows results with $E_{collagen}$ = 30 GPa.   When raising collagen's elastic modulus this high, we see a marked increase in the slope of each line, and therefore a greater increase in the property of bone.   Although, when getting further away from the zero degree orientation (i.e., the 60° orientation) the values for the stiffness of bone are very similar to previous values with the softer collagen.   This is due to the high degree of orientation for each concentric lamella.

2.   Constant Hydroxyapatite Elastic Modulus

Figures 22-24 show the elastic modulus of bone when the lamellae are oriented at various angles and the elastic modulus of hydroxyapatite is kept constant.   With all three figures we see the same trend of bone stiffness, and

realize that the major contributor to its properties are
that of collagen. Note the striking similarities between
figures 22, 23, and 24.

E bone effected by lamella angles (E apatite = 450 Gpa)

Figure 22.   Bone Elastic Modulus with $E_{apatite}$ = 450 GPa

        Figure 22 shows the specific case of $E_{apatite}$ = 450 GPa.
As in the previous figures we see a decreasing trend of the
elastic modulus of bone as the degree of orientation gets
greater and greater. This is again due to the greater
distance from the longitudinal orientation.

E bone effected by lamella angles (E apatite = 550 Gpa)
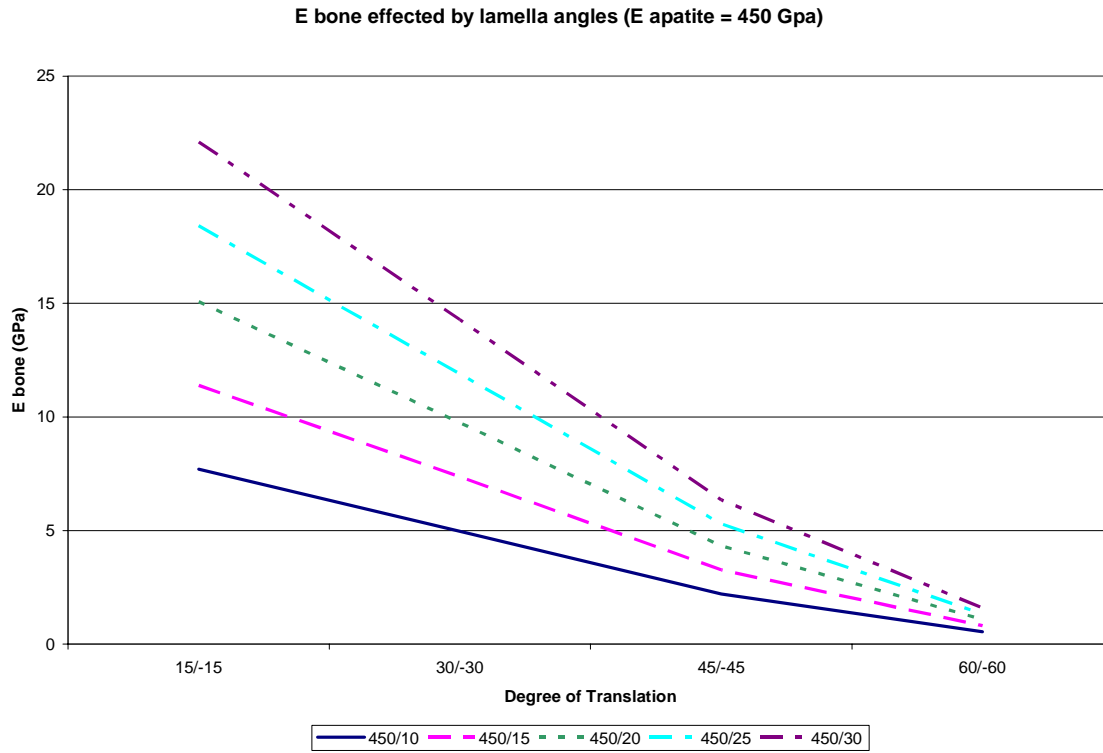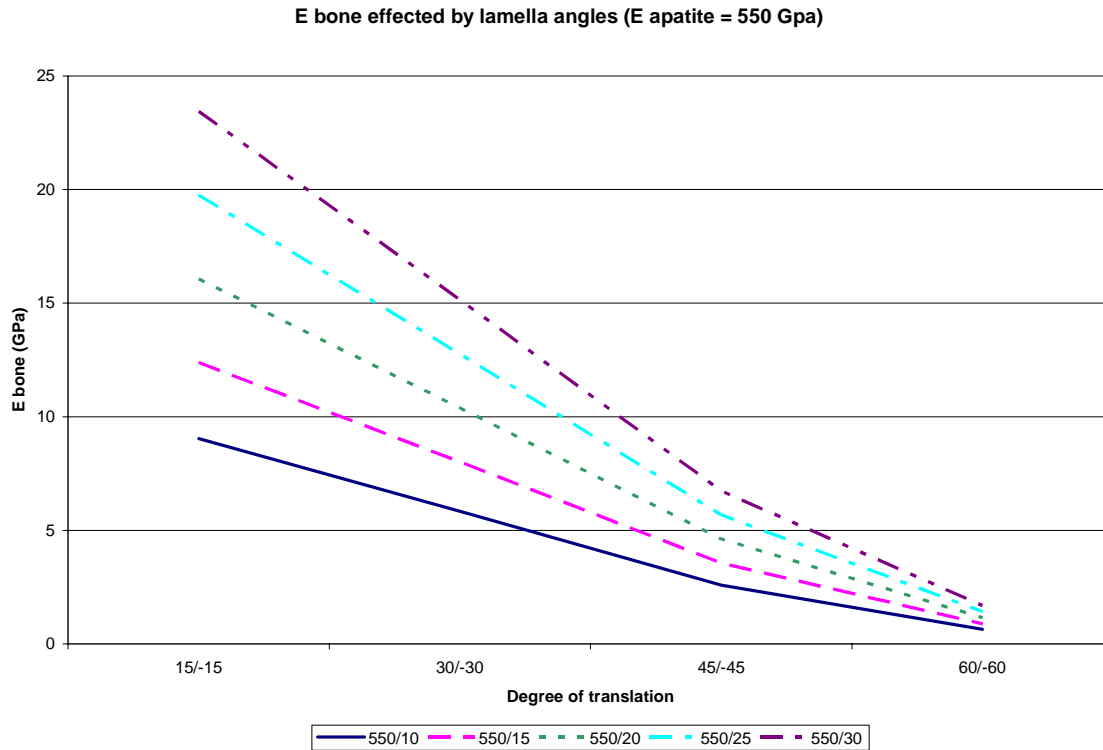

Figure 23.   Bone Elastic Modulus with $E_{apatite}$ = 550 GPa

Figure 23 shows the specific case of $E_{apatite}$ = 550 GPa. Remarkably similar to Figure 22, providing an example of how the properties of bone are not reliant on the properties of hydroxyapatite, but instead on the properties of collagen.

Figure 24 depicts the same trend in results, but with $E_{apatite}$ = 650 GPa.

E bone effected by lamella angles (E apatite = 650 GPa)

Figure 24.   Bone Elastic Modulus with $E_{apatite}$ = 650 GPa

V.   CONCLUSIONS AND RECOMMENDATIONS

A.   CONCLUSIONS

The objective of this study was to derive an analytic model of the basic hierarchical structure of the human bone.   The model computed the stiffness of composite collagen fibers comprised of collagen fibrils and hydroxyapatite mineral crystals. Next, the stiffness of the concentric lamella was computed utilizing the stiffness of t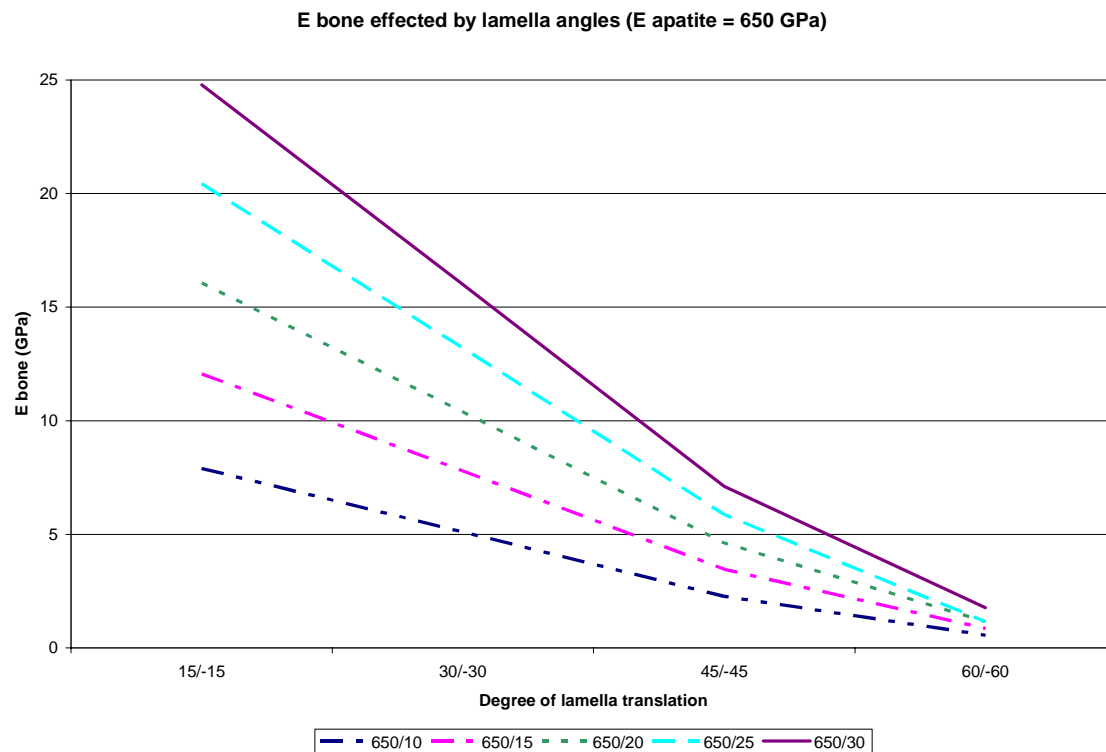he collagen fibers and layer information.   Finally, the effective stiffness of the bone was estimated.   In order to determine the stiffness of the collagen fiber and validate the analytic model, a three-dimensional finite element model was developed.   Once the model was validated, a series of parametric studies were conducted to understand what parameter(s) affected the stiffness of the bone most significantly.

The results of the parametric study demonstrate that the elastic modulus of collagen is much more vital in determining the stiffness of bone than is the elastic modulus of hydroxyapatite.   Both materials had a relatively similar effect on the stress concentration of the composite fiber.   Therefore, if one were to construct an artificial human bone they would need to pay close attention to the material used to replicate collagen, and should not be so concerned about the material used for hydroxyapatite. Another important result, was that the lower the degree of orientation from the centerline, the higher the elastic modulus of bone.   But what was not analyzed in this study was the effect of torsion on the bone stiffness.   To combat

35

the effects of torsion, would require a higher degree of orientation of the lamella.

B.   RECOMMENDATIONS

The following recommendations for future research include:

The current finite element model was analyzed for the axial load. Future work could consist of analyzing the model with different loading conditions including a torsional and a bending load.

This research utilized the elastic modulus of hydroxyapatite and collagen in determining the elastic modulus of bone. In the future, other bone properties such as the transverse modulus and shear modulus could be analyzed to determine if the same trends occur. The interface strength between the collagen and apatite could be another important parameter to analyze.

APPENDIX A - LONGITUDINAL ELASTIC MODULUS OF COMPOSITE FIBER MATLAB PROGRAM

```
%This program is used to calculate the total stiffness
%coefficient for one section of collagen fiber (with
%apatite) as well as the Elastic Modulus of the composite
%fiber.
%      -----^^^^^-----^^^^^-----^^^^^-----
%           k1        k2        k3
%Theory
%1/k = 1/k1 + 1/k2 + 1/k3
%1/k = (k2k3 + k1k3 + k1k2)/(k1k2k3)


clear
clc


r = 60e-9;         %radius in meters
Ec = 10e9;         %Modulus of collagen in Pascals (N/m^2)
L1 = 8e-9;         %length of initial and final section of
collagen in meters
L2 = 48e-9;        %length of apatite in meters
n = 12;            %nr of pieces of apatite around
circumference
Aa = 4.97955e-9*4*2e-9;      %Area of apatite crystal (edge
length*4*width)
Ea = 700e9;        %Modulus of apatite in Pascals (N/m^2)
L = 2*L1 + L2;   %Total length of composite


%k1 = (AE/L1)
k1 = (pi*r^2*Ec)/L1;


alpha = 0.25;


%k2 = k21 + k22 (collagen + apatite)
```

```matlab
%k2 = (AE/L)c + (AE/L)a
k2a = alpha*(n*Aa*Ea)/L2;
k2c = (pi*r^2*Ec)/L2;
k2 = k2a + k2c;
k3 = k1;


k = (k1*k2*k3)/((k1*k2) + (k2*k3) + (k1*k3));


%k = (AE/L)total
Ecomposite = ((k*L)/(pi*r^2))
```

APPENDIX B – ELASTIC MODULUS OF COMPOSITE FIBER ORIENTED AT DIFFERENT ANGLES MATLAB PROGRAM

```matlab
%To determine modulus of elasticity for collagen at 15, 30,
%45, 60, -15, -30, -45, -60 degree angles.


clc
clear


nu = 0.3;
Efiber = 33e9;
data = [];
i=0;


%Try angles of 15,30,45,60,-15,-30,-45,-60 degrees


for theta = [(pi/12) (pi/6) (pi/4) (pi/3) (-pi/12) (-pi/6)
(-pi/4) (-pi/3)];
        Q11 = Efiber/(1-nu^2);
        Q11bar = Q11*(cos(theta))^4;
        Q12bar = Q11*(sin(theta))^2*(cos(theta))^2;
        Q22bar = Q11*(sin(theta))^4;
        Q16bar = Q11*(sin(theta))*(cos(theta))^3;
        Q26bar = Q11*(sin(theta))^3*(cos(theta));
        Q66bar = Q11*(sin(theta))^2*(cos(theta))^2;
%Qbar = [Q11bar Q12bar Q16bar; Q12bar Q22bar Q26bar; Q16bar
Q26bar Q66bar];
        Qbar = zeros(3,3); %Set matrix of zeros as most
%values are assumed zero
        Qbar(1,1) = Q11bar;          %Force value for (1,1)
        Qbar(2,2) = Q22bar;          %Force value for (2,2)
        theta
        Qbar;
```

```matlab
    S11 = 1/Qbar(1,1);
    S22 = 1/Qbar(2,2);
    E1bar = 1/S11                  %Value for E1
    E2bar = 1/S22;                 %Value for E2
    i = i+1;
    data = [data; Q11bar Q22bar];
%   disp(['   Q11bar     Q22bar']);
    data;

end
```

APPENDIX C – LAMELLA AND BONE ELASTIC MODULUS MATLAB PROGRAM

```
%Assuming that there are 12 layers of collagen which make
%up the lamella and that each layer is 120 nm thick.  Take
%the values for E from the "transformedmatrix" m-file for
%various angles.


clc
clear

%theta = pi/12 (15 degrees)
E1bar15 = 31.568e+09;
E1barn15 = E1bar15;


%theta = pi/6 (30 degrees)
E1bar30 = 20.398e+09;
E1barn30 = E1bar30;


%theta = pi/4 (45 degrees)
E1bar45 = 9.0659e+009;
E1barn45 = E1bar45;


%theta = pi/3 (60 degrees)
E1bar60 = 2.2665e+009;
E1barn60 = E1bar60;


%radius calculations for each of 12 layers (assuming radius
%of each layer is equivalent to diameter of a single
%collagen fiber)
r1 = 60e-9;
r2 = r1 + 120e-9;
r3 = r2 + 120e-9;
```

```matlab
r4 = r3 + 120e-9;
r5 = r4 + 120e-9;
r6 = r5 + 120e-9;
r7 = r6 + 120e-9;
r8 = r7 + 120e-9;
r9 = r8 + 120e-9;
r10 = r9 + 120e-9;
r11 = r10 + 120e-9;
r12 = r11 + 120e-9;

%Area calculations for each layer
A1 = pi*r1^2;
A2 = pi*(r2^2-r1^2);
A3 = pi*(r3^2-r2^2);
A4 = pi*(r4^2-r3^2);
A5 = pi*(r5^2-r4^2);
A6 = pi*(r6^2-r5^2);
A7 = pi*(r7^2-r6^2);
A8 = pi*(r8^2-r7^2);
A9 = pi*(r9^2-r8^2);
A10 = pi*(r10^2-r9^2);
A11 = pi*(r11^2-r10^2);
A12 = pi*(r12^2-r11^2);

%Total area of lamella
Atotal = pi*r12^2;
Atotalsum = A1+A2+A3+A4+A5+A6+A7+A8+A9+A10+A11+A12;

%Total Modulus of Elasticity (E1)

%Try opposite layers (15,-15,15,-15...)
```

```
E1total15=(A1*E1bar15)+(A2*E1barn15)+(A3*E1bar15)+(A4*E1bar
n15)+(A5*E1bar15)+(A6*E1barn15)+(A7*E1bar15)+(A8*E1barn15)+
(A9*E1bar15)+(A10*E1barn15)+(A11*E1bar15)+(A12*E1barn15))/A
total;
```

```
%Multiply by 0.7 to account for 70% of bone
```
```
E1bone15 = E1total15*.7
```

```
%Try opposite layers (30,-30,30,-30...)
```
```
E1total30=((A1*E1bar30)+(A2*E1barn30)+(A3*E1bar30)+(A4*E1ba
rn30)+(A5*E1bar30)+(A6*E1barn30)+(A7*E1bar30)+(A8*E1barn30)
+(A9*E1bar30)+(A10*E1barn30)+(A11*E1bar30)+(A12*E1barn30))/
Atotal;
```

```
%Multiply by 0.7 to account for 70% of bone
```
```
E1bone30 = E1total30*.7
```

```
%Try opposite layers (45,-45,45,-45...)
```
```
E1total45=(A1*E1bar45)+(A2*E1barn45)+(A3*E1bar45)+(A4*E1bar
n45)+(A5*E1bar45)+(A6*E1barn45)+(A7*E1bar45)+(A8*E1barn45)+
(A9*E1bar45)+(A10*E1barn45)+(A11*E1bar45)+(A12*E1barn45))/A
total;
```

```
%Multiply by 0.7 to account for 70% of bone
```
```
E1bone45 = E1total45*.7
```

```
%Try opposite layers (60,-60,60,-60...)
```
```
E1total60=((A1*E1bar60)+(A2*E1barn60)+(A3*E1bar60)+(A4*E1ba
rn60)+(A5*E1bar60)+(A6*E1barn60)+(A7*E1bar60)+(A8*E1barn60)
+(A9*E1bar60)+(A10*E1barn60)+(A11*E1bar60)+(A12*E1barn60))/
Atotal;
```

```
%Multiply by 0.7 to account for 70% of bone
```
```
E1bone60 = E1total60*.7
```

```
%Try random layers (15,-15,30,-30,45,-45,15,-15,30,-30,45,-
%45)

E1totalr1=((A1*E1bar15)+(A2*E1barn15)+(A3*E1bar30)+(A4*E1ba
rn30)+(A5*E1bar45)+(A6*E1barn45)+(A7*E1bar15)+(A8*E1barn15)
+(A9*E1bar30)+(A10*E1barn30)+(A11*E1bar45)+(A12*E1barn45))/
Atotal;


%Multiply by 0.7 to account for 70% of bone

E1boner1 = E1totalr1*.7


%Try random layers (45,-45,60,-60,45,-45,60,-60,45,-45,60,-
%60)

E1totalr2=((A1*E1bar45)+(A2*E1barn45)+(A3*E1bar60)+(A4*E1ba
rn60)+(A5*E1bar45)+(A6*E1barn45)+(A7*E1bar60)+(A8*E1barn60)
+(A9*E1bar45)+(A10*E1barn45)+(A11*E1bar60)+(A12*E1barn60))/
Atotal;


%Multiply by 0.7 to account for 70% of bone

E1boner2 = E1totalr2*.7
```

LIST OF REFERENCES

Apatite: Mineral Information Page (2001). Gem and Mineral Miners Inc.
<http://www.mineralminers.com/html/apaminfo.htm> Jul 2002.

Caceci, T (2001). Exercise 8: Bone, Example: Osteon.
<http://education.vetmed.vt.edu/curriculum/VM8054/Labs/Lab8/Lab8.htm> Jul 2002.

Callister Jr. W D (2000). *Materials Science and Engineering an Introduction*. Fifth Edition. New York, John Wiley & Sons Inc.

Collagen, The Columbia Encyclopedia (2001). Comlumbia University Press.
<http://www.bartleby.com/65/co/collagen.html> Jul 2002

Craig Jr. R R (2000). *Mechanics of Materials*. Second Edition. New York, John Wiley & Sons Inc.

Jones R M (1975). *Mechanics of Composite Materials*. Washington D.C., Scripta Book Company.

Osteon: Introduction (2002). SLIBS Bone Website.
<http://www.trinity.edu/rplyston/bone/intro2.htm> Jul 2002.

Rockwood and Green (2001). *Rockwood and Green's Fractures in Adults*. Fifth Edition. Philadelphia, Lippincott Williams & Wilkins.

Ugural A C, Fenster S K (1995). *Advanced Strength and Applied Elasticity*. Third Edition. New Jersey, Prentice Hall PTR.

THIS PAGE INTENTIONALLY LEFT BLANK

INITIAL DISTRIBUTION LIST

1.   Defense Technical Information Center
     Fort Belvoir, VA

2.   Dudley Knox Library
     Naval Postgraduate School
     Monterey, CA

3.   Professor Young W. Kwon ME/KW
     Department of Mechanical Engineering
     Naval Postgraduate School
     Monterey, CA

4.   Mechanical Engineering Program Officer (Code 74)
     Naval Postgraduate School
     Monterey, CA